

Research Article

Study on Influence of Moisture Content on Strength and Brittle-Plastic Failure Characteristics of Xiashu Loess

Yanran Hu ^{1,2}, Shaorui Sun ¹, and Kai Li ¹

¹School of Earth Sciences and Engineering, Hohai University, Nanjing 211111, China

²School of Architectural Engineering, Tongling University, Tongling 244000, China

Correspondence should be addressed to Shaorui Sun; ssrfish@hhu.edu.cn

Received 27 February 2023; Revised 13 April 2023; Accepted 19 April 2023; Published 25 April 2023

Academic Editor: Navaratnarajah Sathiparan

Copyright © 2023 Yanran Hu et al. This is an open access article distributed under the Creative Commons Attribution License, which permits unrestricted use, distribution, and reproduction in any medium, provided the original work is properly cited.

To reveal the influence of water content on the strength characteristics and brittle-plastic failure process of Xiashu loess, the direct shear test and unconfined compressive strength test of Xiashu loess with different water content were carried out, and the influence of water content on its strength characteristics and brittle-plastic failure transformation characteristics was studied. Eight kinds of Xiashu loess with different moisture contents were designed, and a direct shear test and uniaxial compression test were carried out, respectively. The results show that with the increase in water content, the shear strength and unconfined compressive strength of Xiashu loess decrease continuously. The influence of water content on cohesion in the shear strength index is greater than that of the internal friction angle. The relationship curve between cohesion and internal friction angle and water content shows obvious segmentation. When approaching the optimal water content, the downward trend is slowed down. When the water content is constant, the shear strength of the sample will also increase with the increase of normal stress. When the water content is 12% to 15%, the failure mode of Xiashu loess is a brittle failure, and the unconfined compressive strength decreases by 43.23%. When the water content is 15% to 16%, the failure mode of Xiashu loess is a transitional failure, and the unconfined compressive strength decreases by 60.38%. When the water content is greater than 16%, Xiashu loess shows plastic failure, and the unconfined compressive strength decreases slightly.

1. Introduction

The Xiashu loess, also known as the silty clay of the Xiashu Formation, is gray-yellow or brown-yellow. The primary minerals are mainly quartz and feldspar, and the clay minerals are mainly illite. There are many theories about its genesis [1–4] and formation [5, 6], but the eolian theory has gradually dominated and been accepted by most researchers. Xiashu loess has significant water sensitivity [7–9] and weak expansion [10]. It expands with water and shrinks with water loss. These water properties lead to the change of strength and failure mode under rainfall conditions, which greatly increases the difficulty of slope stability evaluation. In addition, Xiashu loess is widely distributed in the middle and lower reaches of the Yangtze River in China, especially in Nanjing and Zhenjiang of Jiangsu [11, 12]. In the engineering construction of these areas, the evaluation of the

strength and failure characteristics of the Xiashu loess slope is unavoidable. It is necessary to understand the physical and mechanical properties of Xiashu loess and its strength and failure characteristics under different water contents reasonably and comprehensively. It has important theoretical and practical engineering significance for building safety and slope stability evaluation in the Xiashu loess area [13–15].

Scholars have carried out a lot of detailed analysis and research on the physical and mechanical properties of Xiashu loess through regression analysis [16], on-site acoustic detection technology [17], laboratory tests [18–21], and numerical tests [22–24]. Han et al. [25] carried out experimental research on the physical properties, water physical properties, and mechanical properties of Nanjing Xiashu loess under different water contents and discussed the main water sensitivity characteristics of Xiashu loess. Shi et al. [26] studied the influence of water content on the shear

strength of Xiashu loess under different shear modes. The results show that the influence of water content is different in different shear modes. In the fast shear test, the water content has a great influence on the shear strength of Xiashu loess. Gu et al. [27] carried out the no-load expansion test of Xiashu loess-bentonite under different initial water content (10%~20%) conditions and found that the initial water content is an important factor affecting the expansion of Xiashu loess-bentonite mixed soil. The higher the initial water content, the smaller the expansion of the sample. Han et al. [28] measured the deformation characteristics and water-holding characteristics of Xiashu loess under different net confining pressures by using the modified GDS unsaturated soil triaxial apparatus and systematically studied the soil-water-mechanical properties of Xiashu loess in Nanjing under dehumidification. It was found that the deformation characteristics of Xiashu loess were affected by net confining pressure and matrix suction. Liu et al. [29] carried out an experimental study on the evolution law of shear strength of Xiashu loess under rainfall infiltration through the data of water content change and analyzed the stability change law of Xiashu loess slope after rainfall infiltration based on the finite element strength reduction method. Xiashu loess has poor water permeability and belongs to a low permeability medium. Hu [30], Li [31], and Sun and Zhao [32] discussed the possibility of using Xiashu loess as an antiseepage cushion in landfill systems by testing and improving it.

From previous studies, it can be found that water content has a great influence on the strength and deformation properties of Xiashu loess. There are relatively many studies on the shear strength of Xiashu loess under different water content, but there are few studies on the comprehensive analysis of the strength and deformation failure characteristics of Xiashu loess, especially the brittle-plastic failure of Xiashu loess under a certain water content. In this study, the basic physical properties of Xiashu loess are measured by indoor geotechnical tests. On this basis, direct shear tests and unconfined compressive strength tests are carried out on Xiashu loess samples with different water contents. The strength and failure characteristics of Xiashu loess under different water contents are comprehensively analyzed. The brittle failure and the transformation characteristics of the brittle-plastic failure of Xiashu loess are analyzed emphatically, which provides an important reference for the relationship between water sensitivity and failure characteristics of Xiashu loess.

2. Materials and Tests

2.1. Basic Characteristics of Test Soil. Xiashu loess was collected from the slope near Huwu Expressway in Jurong City, Zhenjiang City, Jiangsu Province. The soil samples were grayish-yellow-yellowish brown. The basic physical properties of the soil will directly affect the engineering properties of the soil. We did a series of geotechnical tests, such as particle analysis tests, specific gravity tests, boundary water content tests, compaction tests, free expansion rate tests, and permeability tests. According to the test data and referring to

TABLE 1: Particle size distribution table.

Grain size (mm)	Percentage composition (%)
<0.002	1.14
0.002~0.005	72.45
0.005~0.075	6.55
>0.075	19.86

the relevant specifications [33, 34], we can judge that the Xiashu loess used in the test is weakly expansive silty clay. The basic physical properties of the test soil samples are shown in Tables 1 and 2.

2.2. Sample Preparation. The soil sample was dried, crushed with a wooden hammer, and passed through a 2 mm sieve. According to different water content requirements, enough soil sample was placed in a nonabsorbent tray, and the required water was evenly sprayed on the surface of the soil sample with a sprayer. After mixing evenly, it was sealed into a glass tank and wetted for 24 hours to make the soil and water mix evenly. According to the plastic limit and optimal moisture content of Xiashu loess, the moisture content is set to 12%, 13%, 14%, 15%, 16%, 17%, 18%, and 19%. The specimen used in the shear strength test was 61.8 mm in diameter and 20 mm in height. The diameter of the specimen used in the unconfined compressive strength test is 39.1 mm and the height is 80 mm. The preparation of the sample adopts the self-developed hydraulic soil sample preparation instrument, and the required unsaturated soil sample is poured into the mold. After the static pressure is pressed to the required height, it is pushed out with a sample pusher. The Xiashu loess is silty clay, which needs to be added three times. Add the next layer of soil after layered compaction.

2.3. Shear and Compression Tests. To study the influence of different water content on the shear strength of Xiashu loess, six groups of remolded samples with different water content were prepared. The Xiashu loess is fine-grained soil with poor permeability. The ZJ-type strain-controlled quadruple direct shear apparatus shown in Figure 1(a) is used to determine the shear strength index by the direct fast shear test. Normal stresses of 100 kPa, 200 kPa, 300 kPa, and 400 kPa were applied to four specimens in each group, and the shear rate was set to 0.08 mm/min. When the shear stress reading reaches the peak or there is a significant retreat, the test ends; if there is no obvious peak, the test will be stopped when the shear deformation is 6 mm.

There are often free surfaces in practical projects such as slopes and roadbeds. The rock and soil bodies in this part have no lateral constraints and may collapse and slide, and there are certain safety hazards. Therefore, the unconfined compressive strength is used to characterize the ability of rock and soil to resist compression failure under this condition. The YYW-2 strain-controlled unconfined pressure gauge used in the test is shown in Figure 1(b). A thin layer of vaseline was applied to the surface of the prepared sample and placed on the lower-pressure plate. The lower-pressure plate was raised by shaking the wheel until the sample was in

TABLE 2: Basic physical properties parameters of Xiashu loess.

G_s	Liquid limit (%)	Plastic limit (%)	Free swelling ratio (%)	Optimum moisture content (%)
2.73	30.01	15.47	48.85	16.14

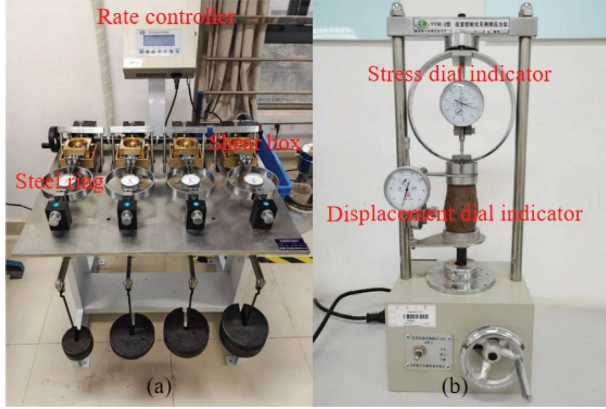


FIGURE 1: (a) Strain-controlled direct shear apparatus and (b) YYW-2 unconfined pressure gauge.

contact with the upper-pressure plate, and the reading of the dial indicator was zeroed. Start the instrument to control the rising speed of the lower-pressure plate at 1%~3% axial strain per minute. When the axial strain is less than 3%, the axial stress and axial strain are measured for every 0.5% increase in axial strain. When the axial strain reaches 3%, the axial stress and axial strain are measured once for every 1% increase in axial strain. If the axial stress reaches the peak, then 3%~5% axial strain can terminate the test; if there is no obvious peak, the test should be carried out to 20% axial strain.

3. Results and Analysis of Laboratory Test

According to the test results, the water sensitivity characteristics of Xiashu loess are analyzed from three aspects: strength, mechanical parameters, and brittle-plastic failure characteristics. The relationship between water sensitivity and brittle-plastic failure characteristics of Xiashu loess was studied.

3.1. Influence of Moisture Content on Strength of Xiashu Loess

3.1.1. Influence of Water Content on Shear Strength of Xiashu Loess. According to the data obtained from the test, the relationship curve between shear stress and shear displacement of Xiashu loess samples with different water content under different normal stresses is drawn, as shown in Figure 2. When the water content is 12%~14%, under the condition of normal stress of 100 kPa, the shear stress of the sample reaches the peak value. With the increase of shear displacement, the shear stress will show a more obvious decreasing trend and then gradually tends to be stable, showing “softening” shear failure. However, due to the remolded sample, the original structure of the soil was

destroyed, the strength changed, and only the friction and cementation between the particles remained, so the peak value of the shear displacement and shear stress curve was not obvious. When the normal stress or water content increases, the shear displacement and shear stress curves do not peak, but gradually tend to be stable after reaching a certain degree, showing “hardening” shear failure.

The relationship between shear strength and normal stress of samples with different water content is shown in Figure 3. When the normal stress is constant, the shear strength of the sample decreases with the increase in water content. When the normal stress is 100 kPa, the shear strength decreases by 80.3%. When the normal stress is 400 kPa, the shear strength decreases by 66.6%. This shows that with the increase of normal stress, the influence of water content on shear strength is gradually weakened. When the moisture content is constant, the effective stress between soil particles will increase with the increase of normal stress, so the shear strength of the sample will also increase. When the water content is 12%, the normal stress increases from 100 kPa to 400 kPa and the shear strength increases by 49.7%. When the water content is 19%, the increase is 155%. This shows that with the increase in water content, normal stress has a significant effect on the improvement of shear strength. The change of shear strength in the range of lower water content is greater than that of higher water content. When the water content is 14%~16% and 18%~19%, the shear strength curve is denser, indicating that the change is relatively small.

3.1.2. Effect of Water Content on Unconfined Compressive Strength of Xiashu Loess. The relationship curve between axial stress and axial strain under different water content conditions is drawn, as shown in Figure 4. From the diagram, the stress-strain curve trend of the experimental group and the control group is the same, and the difference in the unconfined compressive strength obtained is small, indicating that the test results are accurate and reliable.

When the axial stress is applied at the beginning, the stress-strain curve is slightly concave, indicating that the sample is in the compaction stage. At this time, the stress applied to the sample is small, but it is enough to make the distance between the blocks in the soil gradually narrow and the contact area increase. At the same time, part of the gas in the pores is discharged outward under extrusion, and the relative proportion of the solid phase in the soil is further increased.

After the compaction stage, the sample begins to enter the elastic deformation stage, and the axial stress-axial strain is linearly related. The slope of the straight line at this stage is the elastic modulus of the soil. The analysis shows that the slope of the straight line gradually decreases with the

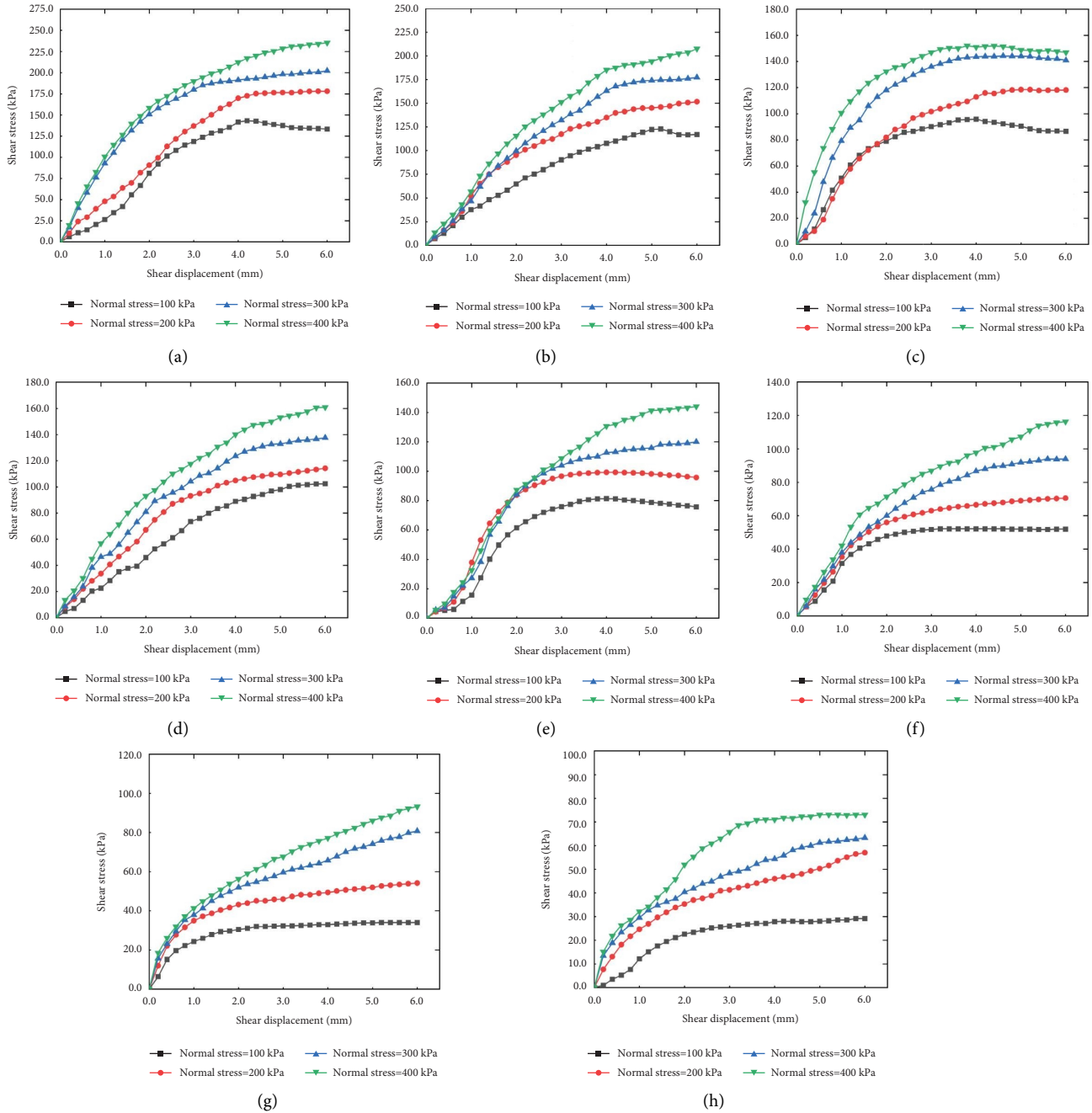


FIGURE 2: Shear stress-shear displacement curve of Xiashu loess under different water content. (a-h) Water content 12~19%.

increase in water content. The elastic modulus decreases with the increase in water content. This shows that the ability of the sample to resist elastic deformation is gradually weakening. When the water content is close to 16%, the deceleration of the linear slope begins to decrease, and the decrease of the elastic modulus becomes smaller. Then, the specimen enters the yield stage, the axial stress-axial strain curve bulges outward, and the growth rate of axial stress gradually decreases. Through the analysis of the deformation and failure process of the comprehensive sample, the sample began to bulge at this stage, and there were tiny cracks.

After that, the axial stress-axial strain curves of samples with different moisture contents began to show different trends. After the peak value of the sample curve with water content less than 16%, the axial stress decreases sharply with the increase of the axial strain, showing the strain softening characteristics. In this moisture content range, the axial strain corresponding to the peak value gradually increases, and the decrease of axial stress after the peak value is relatively moderate. When the water content of the sample is 12%, the axial strain corresponding to the peak is about 4.50%, and when the water content is 15%, the

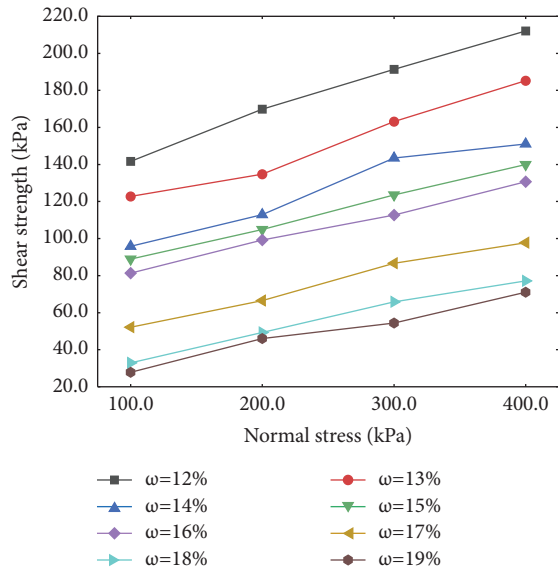


FIGURE 3: Shear strength-normal stress relationship curve of Xiashu loess under different water content.

corresponding axial strain increases to 14.50%, which is more than twice the former. After reaching the peak value, the axial stress did not suddenly decrease to the residual strength but decreased along the oblique line. With the increase in water content, the decline process became more and more moderate. The increase in water content also makes the stress concentration in the soil gradually insignificant, and the duration of the sample from the development of cracks to shear failure gradually increases.

Figure 5 is the relationship curve between unconfined compressive strength and the water content of Xiashu loess. It can be seen from the diagram that under the condition of a certain dry density, the unconfined compressive strength will decrease with the increase in water content. When the water content increases from 12% to 19%, the unconfined compressive strength decreases from 418.21 kPa to 46.53 kPa, with a decrease of 88.87%. When the moisture content increased from 12% to 16%, the unconfined compressive strength decreased by 324.15 kPa, a decrease of 77.51%. When the water content increased from 16% to 19%, the unconfined compressive strength decreased by 47.53 kPa, with a decrease of 50.53%, indicating that the decrease rate of unconfined compressive strength gradually decreased.

In the case of low water content, clay minerals in the soil adsorb water molecules, making them firmly attached to the surface of the soil particles to form a strong-bound water film. Strongly bound water has a greater viscosity than ordinary water, and its properties are similar to solid. When water molecules adsorb with clay minerals and microcrystalline-free iron oxide to form a stable aggregate structure, the intermolecular attraction increases, and the cementation of clay minerals itself can inhibit the extrusion to a certain extent. Therefore, it has a strong antideformation ability and relatively high unconfined compressive strength. When the water content increases, the weakly bound water

film becomes thicker and water is filled between the pores. This increases the distance between the aggregates and reduces the attraction between the molecules. When the pore water pressure is generated, it will offset part of the compaction. The cement between the particles began to dissolve, the cementation became weak, and the unconfined compressive strength began to decrease. When the water content increases to a certain extent, the dissolution rate of the cement decreases, and the attenuation of the unconfined compressive strength gradually tends to be gentle.

3.2. Relationship between Moisture Content and Shear Strength Parameters of Xiashu Loess. The shear strength parameters of Xiashu loess are composed of cohesion and internal friction angle. Figure 6 shows the relationship between cohesion, internal friction angle, and water content. When the moisture content is in the range of 12%~19%, with the increase of moisture content, the cohesion decreases from 120.55 kPa to 15.33 kPa, a decrease of 87.29%. When the moisture content is in the range of 12%~14% and 17%~18%, the average decrease of cohesion is 20.17% and 48.08%, respectively. However, when the moisture content was 15%~16%, the decrease was only 8.12%, and the relationship curve showed a gentle trend.

The cohesive force is mainly formed by the cementation between soil particles and the attraction of electric molecules. When the water content is low, a thin strong-bound water film is formed on the surface of soil particles, which is beneficial to the bonding between particles. The content of quartz in the Xiashu loess of the Ningzhen area is about 70%, and the content of hydromica and feldspar is less. The oxides contained are mainly amorphous iron (FeO) and free alumina (Al_2O_3), both of which have flocculation cementation. When they are attached to the surface of clay minerals in Xiashu loess, they can enhance the adsorption force and reduce the dispersion of clay particles and adhesion between particles. In addition, the iron and aluminum oxides themselves are positively charged and can adsorb anions to change the thickness of the electric double layer. When the water content increases, the cementing material dissolves, the cohesive force between the particles decreases, and the free water between the pores increases. The lubrication of the water film will reduce the friction between the particles and the cohesion of the soil begins to decrease.

The relationship curve between cohesion and water content of Xiashu loess shows obvious segmentation, and the inflection point water content is 14%, 16%, and 19%, respectively. For unsaturated cohesive soil, when the water content is less than the plastic limit, it is generally believed that there is only strong-bound water between pores, which can produce a strong bonding force between particles. When the water content increases and is less than the plastic limit, the weak-bound water begins to appear, the connection of the strong-bound water begins to weaken, and the cohesion will decrease. The plastic limit of Xiashu loess used in the test is 15.47%. When the moisture content begins to approach this value, the increase of the thickness of the weak-bound water film is small, so the decrease of cohesion is slow.

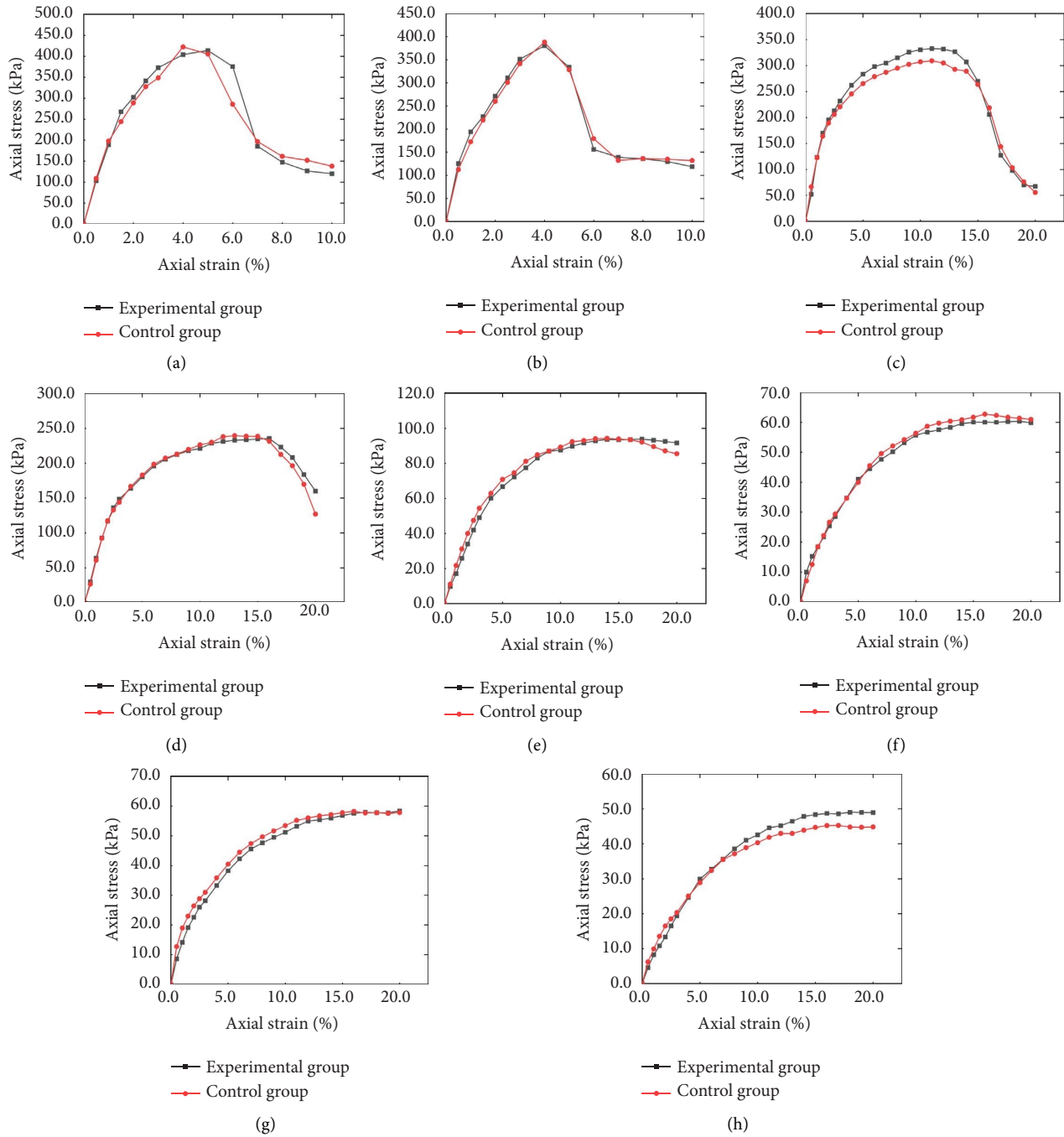


FIGURE 4: Axial stress-strain curves of specimens with different water contents. (a-h) Water content 12~19%.

The internal friction angle decreases with the increase of moisture content, and the relationship curve also shows obvious segmentation, but it is not the same as the change process of cohesion. The moisture content of the first inflection point is 15%, which is different from the first inflection point of the relationship curve between cohesion and moisture content, but it is also close to the plastic limit of Xiashu loess. The water content of the second inflection point is 17%. In the range of water content studied, the third inflection point does not appear. It can be concluded that the inflection point water content of the relationship curve

between the internal friction angle and water content of Xiashu loess is greater than the inflection point water content of the relationship curve between cohesion and water content.

The Xiashu loess is weak expansive soil. When the water content increases, the soil will experience a slight expansion, increasing the contact area between the particles and an increase in the friction force, which offsets a part of the impact caused by the decrease in the connection force of the strong-bound water. Therefore, the reduction of the friction angle within this range is relatively gentle. The expansion

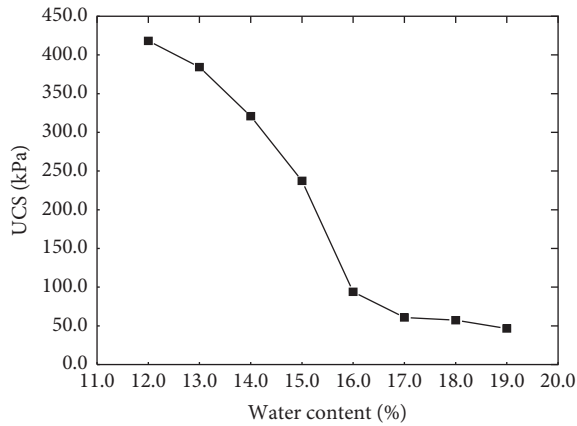


FIGURE 5: Unconfined compressive strength-water content relationship curve.

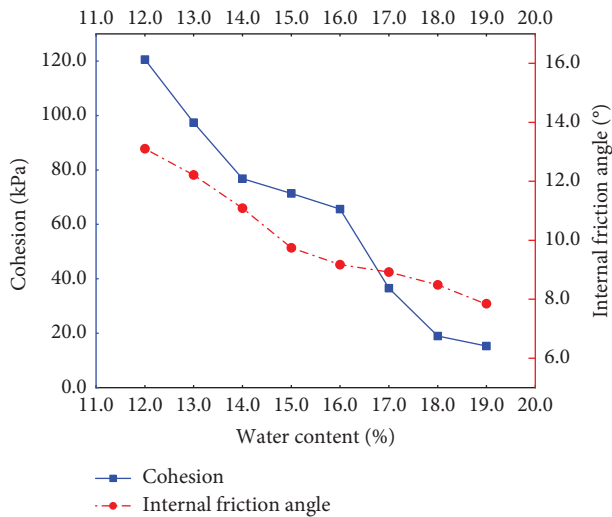


FIGURE 6: Relationship curves of cohesion, internal friction angle, and water content of Xiashu loess.

capacity of Xiashu Loess is limited. When the water content increases again, the connecting force of strong-bound water decreases significantly, the lubrication effect of pore water becomes stronger, and the friction angle decreases greatly.

From the analysis of the mineral composition, with the increase of water content, the cohesion of illite will continue to decrease, while the internal friction angle is slightly affected. The relationship between cohesion and moisture content of montmorillonite is similar to that of illite, but the internal friction angle will be stable within a certain range of moisture content. When the growth of moisture content exceeds this range, the internal friction angle gradually decreases. The relationship between cohesion and internal friction angle of kaolinite and water content is relatively simple, and the overall trend is downward. The clay minerals in Xiashu loess are mainly illite (a content of 43%~92%), followed by montmorillonite, kaolinite content is small, so the influence of illite on shear strength is relatively large. It is also because the cohesive force and internal friction angle of

clay minerals are different in sensitivity to water, which makes the cohesive force and internal friction angle of Xiashu loess vary with water content.

3.3. Relationship between Moisture Content and Brittle-Plastic Failure of Xiashu Loess. The stress-strain curve of Xiashu loess has three different shapes as shown in Figure 4. The first is the peak curve. The stress after the peak decreases rapidly to the residual strength, but the strain increases rapidly until failure occurs. The other is when the stress increases to a certain limit, value will no longer increase, but the strain value continues to increase until the damage. The third is between the two. The uniaxial failure mode of Xiashu loess with different water content is shown in Figure 7.

Corresponding to the three different shapes of the curve, Xiashu loess appeared in the following three forms of damage, such as in Figure 8. The first is a brittle failure. When the moisture content is 12%–14%, the soil sample undergoes a very small elastic deformation, and almost no yield process occurs. The deformation of the soil sample failure process is very small, the failure surface is flat and smooth and is splitting type, and the intersection angle with the bottom surface is approximately 45°, belonging to brittle failure. The damaged soil sample lost continuity, and the soil blocks on both sides could not contact stably at the fracture surface.

The second is a transitional failure. When the water content is 15%, the failure mode is the coexistence of brittle failure and plastic failure. When the soil sample is destroyed, it still has a flat failure surface. The failure surface is still relatively smooth, but there are small scratches. The soil sample has a lateral expansion at both ends and small cracks. The crack direction is almost perpendicular to the direction of the failure surface. The soil sample after destruction lost continuity.

The third is a plastic failure. When the moisture content is greater than 16%, the outward bulging and small vertical cracks visible to the naked eye begin to appear in the middle of the sample, and the degree of bulging and the number of cracks, openings, and penetration continue to increase. There is no overall failure of the specimen, but dislocation along the failure surface, which is a plastic failure. After the destruction of the sample, development has many cracks, part of the through conical staggered ups and downs and even smaller soil outward ups and downs.

The types of deformation and failure characteristics of specimens are closely related to water content and have different deformation and failure effects. When the water content is relatively low, the soil suddenly produces large cracks, and there is no obvious sign before the failure, which is sudden and brittle failure occurs. This may also be an important reason for the frequent collapse or kiln collapse disasters in the Xiashu loess area. When the water content is high, small cracks begin to appear on the surface of the sample, and then the cracks continue to expand and finally penetrate the cross section of the sample. The sample finally reaches failure and plastic failure occurs, showing the characteristics of progressive failure. This may also be an

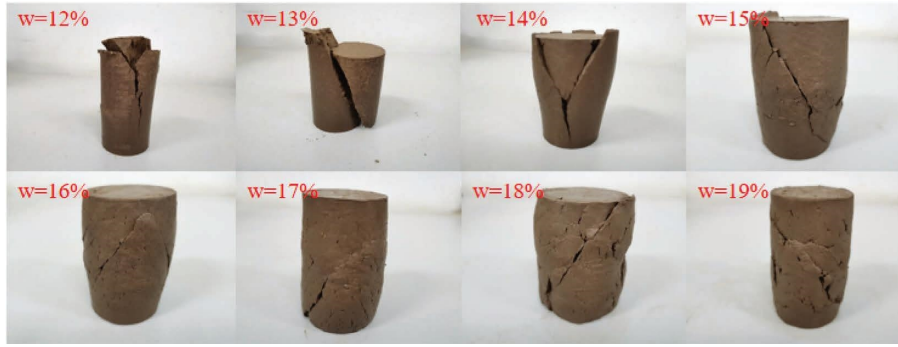


FIGURE 7: The uniaxial failure mode of Xiashu loess with different water content.

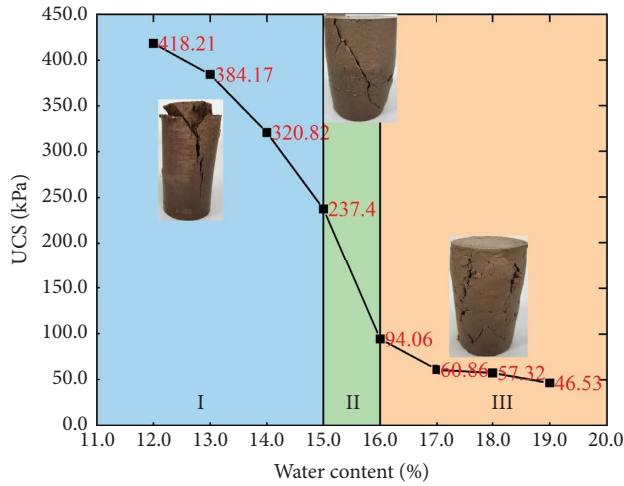


FIGURE 8: Three failure modes of Xiashu loess.

important reason for the progressive failure of the Xiashu loess slope under rainfall infiltration.

4. Conclusion

To study the strength and failure characteristics of Xiashu loess under different water contents, the direct shear test and unconfined compressive strength test of Xiashu loess samples under different water contents were carried out. The effects of water content on shear strength, unconfined compressive strength, shear strength parameters, and elastoplastic failure characteristics of Xiashu loess were comprehensively analyzed. The following conclusions are drawn:

- (1) Through the direct shear test, it is found that with the increase of moisture content, the shear strength of Xiashu loess decreases, the low normal stress decreases by 80.3%, and the high normal stress decreases by 66.6%.
- (2) Compared with the internal friction angle, the cohesion is more affected by the water content. When the water content increases from 12% to 19%, the cohesion decreases by 87.3%, and the internal friction angle decreases by 40%. The water sensitivity of the internal friction angle is stronger than that of cohesion. The relationship curves of cohesion,

internal friction angle, and water content show obvious segmentation. When the two are near the optimal water content, the decline rate decreases sharply and the curve is gentle. When the water content is greater than 18%, the change of cohesion with water content is relatively small, while the change of internal friction angle is still significant.

- (3) In the unconfined compressive strength test, the unconfined compressive strength of Xiashu loess decreases with the increase of initial water content. When the water content increases from 12% to 19%, the unconfined compressive strength decreases by 89%.
- (4) The failure process of Xiashu loess samples with different water content is quite different. When the moisture content is less than 15%, the sample is a brittle failure; when the moisture content is greater than or equal to 16%, the sample is a plastic failure.

Data Availability

All datasets generated during this study are available from the corresponding author upon reasonable request.

Conflicts of Interest

The authors declare that they have no conflicts of interest.

Authors' Contributions

Yanran Hu performed data curation and formal analysis, validated the study, and wrote the original draft. Shaorui Sun conceptualized the study, proposed the methodology, supervised the study, revised the original draft, and performed funding acquisition. Kai Li performed data curation and formal analysis and revised the original draft. All authors have read and agreed to the published version of the study and agreed to be accountable for all aspects of the work.

Acknowledgments

This research was funded by China's Postdoctoral Science Fund (no. 2021M690865) and the open fund of Jiangsu Province Geological Engineering Environment Intelligent Monitoring Engineering Research Center (no. 2021-ZNJKJJ-

04), and this research was supported by the Fundamental Research Funds for the Central Universities (no. B210201002) and Natural Science Foundation of China (nos. 41672258 and 42007256). The research was supported by the Natural Key Projects in Anhui Province (no. 2022AH051751). The authors would like to thank for the fund support by Huilin Le and the methodology by Qian Yin and the supervision by Jihong Wei.

References

- [1] X. Li, Z. Han, H. Lu et al., "Onset of Xiashu loess deposition in southern China by 0.9 Ma and its implications for regional aridification," *Science China Earth Sciences*, vol. 61, no. 3, pp. 256–269, 2018.
- [2] W. Zhang, L. Yu, M. Lu et al., "East Asian summer monsoon intensity inferred from iron oxide mineralogy in the Xiashu Loess in southern China," *Quaternary Science Reviews*, vol. 28, no. 3–4, pp. 345–353, 2009.
- [3] Y. Ren, X. Li, Z. Han et al., "View Correspondence (jump link). The chronological sequence of the Xiashu Loess based on the relative paleointensity of geomagnetic field and its implications (Article)," *Acta Geophysica Sinica*, vol. 63, no. 5, pp. 2024–2035, 2020.
- [4] S. Yi, X. Li, Z. Han, H. Lu, J. Liu, and J. Wu, "High resolution luminescence chronology for Xiashu Loess deposits of Southeastern China," *Journal of Asian Earth Sciences*, vol. 155, pp. 188–197, 2018.
- [5] J. Pang and C. Huang, "Mid-Holocene soil formation and the impact of dust input in the middle reaches of the yellow river, Northern China," *Soil Science*, vol. 171, no. 7, pp. 552–563, 2006.
- [6] X. Wang, H. Lu, H. Zhang et al., "Distribution, provenance, and onset of the Xiashu Loess in Southeast China with paleoclimatic implications," *Journal of Asian Earth Sciences*, vol. 155, pp. 180–187, 2018.
- [7] F. Ma, J. Yang, and X. Bai, "Water sensitivity and micro-structure of compacted loess," *Transportation Geotechnics*, vol. 11, pp. 41–56, 2017.
- [8] P. Sun, M. Zh, L. Feng, S. Wang, X. Dang, and M. Liu, "Water sensitivity of loess and its spatial-temporal distribution on the loess plateau," *Northwestern Geology*, vol. 52, no. 2, pp. 117–124, 2019.
- [9] Y. Leng, J. Peng, S. Wang, and F. Lu, "Development of water sensitivity index of loess from its mechanical properties," *Engineering Geology*, vol. 280, Article ID 105918, 2021.
- [10] J. Xia and A. Han, "Cyclic variability in microstructure and physio-mechanical properties of the Xiashu Loess-palaeosol sequence in Nanjing, China," *Engineering Geology*, vol. 104, no. 3–4, pp. 263–268, 2009.
- [11] P. Qian, X. Zheng, J. Cheng, Y. Han, Y. Dong, and J. Zhang, "Tracing the provenance of aeolian loess in the Yangtze River Delta through zircon U-Pb age and geochemical investigations," *Journal of Mountain Science*, vol. 15, no. 4, pp. 708–721, 2018.
- [12] Y. Chen, X. Li, Z. Han, S. Yang, Y. Wang, and D. Yang, "Chemical weathering intensity and element migration features of the Xiashu loess profile in Zhenjiang, Jiangsu Province," *Journal of Geographical Sciences*, vol. 18, no. 3, pp. 341–352, 2008.
- [13] W. Wang, S. Sun, J. Wei, Y. Yu, W. He, and J. Song, "Numerical experimental study on optimum design of anchorage system for Xiashu loess slope," *Journal of Central South University*, vol. 28, no. 9, pp. 2843–2856, 2021.
- [14] X. Yang, D. Sun, and H. Jing, "Morphological Features of Shear-Formed Fractures Developed in a Rock Bridge," *Engineering Geology*, vol. 278, Article ID 105833, 2020.
- [15] Y. Wu, J. Cui, J. Huang, W. Zhang, N. Yoshimoto, and L. Wen, "Correlation of critical state strength properties with particle shape and surface fractal dimension of clinker ash," *International Journal of Geomechanics*, vol. 21, no. 6, Article ID 04021071, 2021.
- [16] J. Xiao and W. Zheng, "Behaviors of Xiashu loess in the lower reaches of China's Yangtze River under triaxial compression and the microscopic explanations," *Applied Mechanics and Materials*, vol. 858, pp. 91–97, 2016.
- [17] H. Lu, J. Li, W. Wang, and C. Wang, "Cracking and water seepage of Xiashu loess used as landfill cover under wetting-drying cycles," *Environmental Earth Sciences*, vol. 74, no. 11, pp. 7441–7450, 2015.
- [18] S. Sun, W. Wang, J. Wei et al., "The physical-mechanical properties degradation mechanism and microstructure response of acid-alkali-contaminated Xiashu loess," *Natural Hazards*, vol. 106, no. 3, pp. 2845–2861, 2021.
- [19] B. Li, Y. Niu, and T. Miao, "Water sensitivity of malan loess in Lanzhou," *Chinese Journal of Geotechnical Engineering*, vol. 29, no. 2, pp. 294–298, 2007.
- [20] B. Li and T. Miao, "Research on water sensitivity of loess shear strength," *Chinese Journal of Rock Mechanics and Engineering*, vol. 25, no. 5, pp. 1003–1008, 2006.
- [21] Y. Wu, H. Yamamoto, J. Cui, and H. Cheng, "Influence of load mode on particle crushing characteristics of silica sand at high stresses," *International Journal of Geomechanics*, vol. 20, no. 3, Article ID 04019194, 2020.
- [22] J. Xia and X. Chen, "Numerical analysis on soil and rock formation of ancient gravel strata around Nanjing[J]," *Pedosphere*, vol. 11, no. 3, pp. 263–269, 2001.
- [23] L. Han, Q. Hao, Y. Qiao et al., "Geochemical evidence for provenance diversity of loess in southern China and its implications for glacial aridification of the northern subtropical region," *Quaternary Science Reviews*, vol. 212, pp. 149–163, 2019.
- [24] A. Avram, D. Constantin, Q. Hao, and A. Timar-Gabor, "Optically stimulated luminescence dating of loess in South-Eastern China using quartz and polymineral fine grains," *Quaternary Geochronology*, vol. 67, Article ID 101226, 2022.
- [25] A. Han, T. Li, L. Zhang, and H. Xu, "Experimental study on water sensitivity characteristics of Nanjing Xiashu loess," *Journal of Nanjing Tech University (Natural Science Edition)*, vol. 6, pp. 81–86, 2015.
- [26] W. Shi, J. Wei, J. Song, H. Le, and X. Gao, "Study on the influence of moisture content to shear strength tests for Xiashu loess," *Journal of Xihua University (Natural Science Edition)*, vol. 35, pp. 97–101, 2016.
- [27] K. Gu, B. Shi, and C. Tang, "Experimental Study and mechanisms of swelling properties of Xiashu-bentonite mixture," *Hydrogeology & Engineering Geology*, vol. 4, pp. 125–129, 2011.
- [28] A. Han, T. Li, and H. Xu, "Hydro-mechanical behavior of Nanjing Xiashu loess in desorption moisture state," *Journal of Engineering Geology*, vol. 24, no. 2, pp. 268–275, 2016.
- [29] S. Liu, Y. Cai, T. Cheng, P. Zhou, and X. Wang, "Stability analysis of Xiashu loess slope under rainfall infiltration," *Journal of Geological Hazards and Environment Preservation*, vol. 33, pp. 32–37, 2022.

- [30] Y. Hu, "Feasibility study of Xiashu loess as landfill liner," *West-China Exploration Engineering*, vol. 17, no. 2, pp. 220–222, 2005.
- [31] Z. Li, *Study on Fractal Permeability and Percolation Mechanism of Modified Xiashu Loess*, Nanjing Tech University, Nanjing, China, 2007.
- [32] H. Sun and X. Zhao, "Experimental study on improved Xiashu cohesive soil for express railway subgrades," *Chinese Journal of Geotechnical Engineering*, vol. 26, pp. 293–295.
- [33] Government ministry, *Technical code for buildings in expansive soil regions Code for design of building foundation*, Ministry of Housing and Urban-Rural Development of the People's Republic of China, Beijing, China, 2013.
- [34] Government ministry, *Code for design of building foundation (Gb50007-2011)*, Ministry of Housing and Urban-Rural Development of the People's Republic of China, Beijing, China, 2011.